Novel Multifunctional Umbrella Molecule Material Combining Photoelectric Conversion and Second-Order Optical Nonlinearities in Langmuir−Blodgett Monolayers

Fu-You Li,[†,‡] Jie Zheng,[‡] Chun-Hui Huang,*[,‡] Lin-Pei Jin,*[,†] Jin-You Zhuang,[†] Jian-Quan Guo,[†] Xin-Sheng Zhao,[§] and Ting-Ting Liu[§]

Department of Chemistry, Beijing Normal University, Beijing, 100875, P. R. China, State Key Laboratory of Rare Earth Materials Chemistry and Applications, Peking University-The University of Hong Kong Joint Laboratory on Rare Earth Materials and Bioinorganic Chemistry, Peking University, Beijing 100871, China, and Department of Chemistry, Peking University, Beijing 100871, China

Received: October 11, 1999; In Final Form: January 25, 2000

A dipolar two-dimensional multifunctional (D-π)$_3$-A dye molecule, 2,4,6-tris(4-(*N*-methyl-*N*-hexadecylamino)-styryl)pyrylium tetrafluoroborate (P_3) was synthesized. The dye molecule was successfully transferred onto an ITO electrode or quartz by the Langmuir−Blodgett (LB) technique. The second-harmonic generation (SHG) and photoelectric conversion (PEC) properties of the "molecular umbrella" monolayers were studied under 10 and 40 mN m^{-1} surface pressure. The different tilt angle of the "molecular umbrella" results in the difference of SHG and PEC properties. For comparison, dipolar one-dimensional molecule 2,6-dimethyl-4-(4-(*N*-methyl-*N*-hexadecylamino)styryl)pyrylium tetrafluoroborate (P_1) was also investigated. The experimental results show that the SHG and PEC properties of the dipolar two-dimensional molecule (P_3) are better than those of the dipolar one-dimensional molecule (P_1). For example, under favorable conditions (−100 mV, dissolved O_2, 2 mM MV^{2+}, and 4 mM Eu^{3+}), the quantum yields for P_3 and P_1 monolayers (deposited under 40 mN m^{-1}) are 1.21 and 0.42%, respectively.

Introduction

There has been considerable interest recently in the multifunctionalization of molecular materials for their potential use in technologies where several properties need to be combined in the same device. As one of electrooptic materials, organic nonlinear optical (NLO) materials have been extensively studied in the past decades because of their potential applications in the electrooptic signals, telecommunication and data storage.[1−3] Multifunctional NLO materials with other properties, such as magnetism[4,5] and conductivity[6,7] have been already reported. The traditional approach to design of NLO materials has been focused on the one-dimensional extended π-conjugated dipolar system with appended strong electron donors and acceptors.[8−10] Recently, the nondipolar two-dimensional (octupolar) NLO chromophores with 3-fold symmetry have been extensively studied both theoretically and experimentally.[11−13] However, dipolar two-dimensional NLO chromophores have no systematic experimental study yet, though they exhibit several interesting properties.[14,15] The principle of second-order nonlinear optics indicates that the difference in the dipole moment of the molecule between the ground and excited states is one of the main factors for molecular hyperpolarizability.[16] On the other hand, photocurrent generation and charge dissociation are connected with the charge separation process, which also requires a large dipole moment in the excited state. So, it is reasonable to expect that the higher the molecular hyperpolarizability, the better the molecular photoelectric conversion efficiency in some systems. In fact, positive results have been observed.[17] However, in the past few years, we have mainly studied one-dimensional dipolar molecules with a single chromophore such as hemicyanine and its congeners and azopyridinium compounds.[17−23] As a part of our systematic study, we designed a novel dipolar two-dimensional (D-π)$_3$-A dye molecule, 2,4,6-tris(4-(*N*-methyl-*N*-hexadecylamino)styryl)pyrylium tetrafluoroborate (P_3) (Scheme 1), in which three electron-donating groups link one electron-accepting group through three π-conjugation (−CH═CH−) groups. We focused on whether the above relationship between second-harmonic generation (SHG) and photoelectric conversion (PEC) properties still remains in this three chromophores dye.

In this contribution, we report that this multifunctional molecule was successfully transferred onto the indium−tin oxide (ITO) substrate or quartz by the LB technique. The SHG and PEC properties of the dipolar two-dimensional dye LB monolayers were examined. Mechanistic models for photoelectric conversion under different conditions are proposed. For comparison, a dipolar one-dimensional molecule (P_1) was also synthesized and studied under the same conditions.

Experimental Section

4-(*N*-Methyl-*N*-hexadecylamino)benzaldehyde was prepared according to the previous method reported.[24] 2,4,6-Trimethylpyrylium tetrafluoroborate was synthesized as described in the literature.[25] 2,4,6-Tris(4-(*N*-methyl-*N*-hexadecylamino)-styryl)pyrylium tetrafluoroborate (P_3) and 2,6-dimethyl-4-(4-(*N*-methyl-*N*-hexadecylamino)styryl)pyrylium tetrafluoroborate (P_1) were synthesized as follows: In a general procedure, an ethanol solution (10 mL) of 2,4,6-trimethylpyrylium tetrafluoroborate was added to the corresponding molar equivalent of aldehyde. The mixture was refluxed for 5 h. After it was cooled

[†] Beijing Normal University.
[‡] State Key Laboratory of Rare Earth Materials Chemistry and Applications, Peking University-The University of Hong Kong Joint Laboratory on Rare Earth Materials and Bioinorganic Chemistry, Peking University.
[§] Department of Chemistry, Peking University.

10.1021/jp993605u CCC: $19.00
Published on Web 05/04/2000

SCHEME 1: Molecular Structure of the Two Dye Congeners

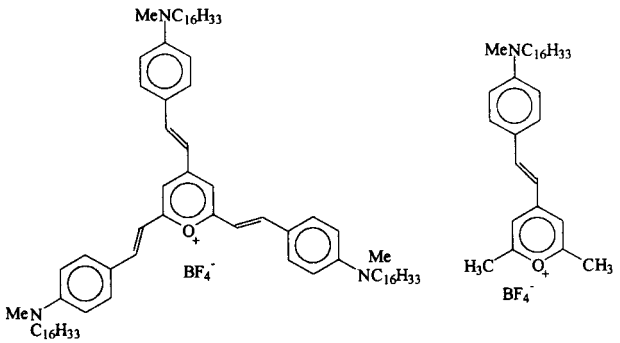

to room temperature, the resulting precipitate was filtered and chromatographed (SiO_2, MeOH:CH_2Cl_2 = 1:8, V/V).

Data for P_3. Yield: 82%. Mp: 241−242 °C. Anal. Calcd for $C_{80}H_{128}N_3OBF_4$: C, 77.80; H, 10.46; N, 3.40. Found: C, 77.84; H, 10.75; N, 3.45. δ_H (300 MHz, $CDCl_3$): 0.88 (t, 9H, $3CH_3$), 1.26 (m, 78H, $39CH_2$), 1.56 (m,6H, $3CH_2$), 2.97 (s, 3H, $1N-CH_3$), 3.04 (s, 6H, $2N-CH_3$) 3.30 (m, 6H, $3N-CH_2$), 6.45 (d, 2H, phenyl), 6.70 (d, 4H, phenyl), 6.75 (d, 2H, 2CH═), 7.20 (d, 1H, 1CH═), 7.27 (s, 2H, pyrylium), 7.36 (d, 2H, phenyl), 7.44 (d, 4H, phenyl), 7.53 (d, 2H, 2CH═), and 7.73 (d, 1H, 1CH═).

Data for P_1. Yield: 74%. Mp: 176−177 °C. Anal. Calcd for $C_{32}H_{50}NOBF_4$: C, 69.70; H, 9.15; N, 2.54. Found: C, 69.65; H, 9.53; N, 2.65. δ_H (300 MHz, $CDCl_3$): 0.87 (t, 3H, $1CH_3$), 1.27 (m, 26H, $13CH_2$), 1.63 (m, 2H, $1CH_2$), 2.60 (s, 6H, $2CH_3$-pyrylium), 3.14 (t, 3H, $1N-CH_3$), 3.46 (t, 2H, $1N-CH_2$), 6.75 (d, 2H, phenyl), 6.89 (d, 1H, 1CH═), 7.47 (s, 2H, pyrylium), 7.59 (d, 2H, phenyl), and 7.72 (d, 1H, 1CH═).

Methylviologen diiodide (MV^{2+}) was synthesized by reaction of 4,4′-dipyridyl with methyl iodide. Its identity was confirmed by ^1H NMR analysis. The electrolyte for the electrochemical experiment was KCl (AR grade, Beijing Chemical Factory, China). Hydroquinone (H_2Q) (AR grade, Beijing Chemical Factory, China) was recrystallized from water before use. $EuCl_3 \cdot 6H_2O$ was obtained by reaction of Eu_2O_3 with hydrochloric acid. The spreading solvent used for monolayer deposition was chloroform (AR grade, Beijing Chemical Factory, China).

C, H, N data of the compounds were obtained by using a Carlo Erba 1106 elemental analyzer. ^1H NMR spectra were measured by using Bruker ARX300. Electronic spectra in solution or on LB monolayers were recorded on a Shimadzu model 3100 UV−vis−NIR spectrophotometer. The melting point measurement was performed on an X4 micromelting point apparatus. The monolayers of P_3 and P_1 were prepared by spreading the corresponding dye solution on a NIMA 622 Langmuir−Blodgett trough. Water from a EASY pure RF system was used as a subphase ($R \sim 18$ MΩ. cm, pH ~ 5.6). All experiments were carried out at a subphase temperature of 20 ± 1 °C. Details on the method used for pressure (π)−area (A) measurement and the transfer process were the same as described previously.[22] In all cases, the transfer ratios were close to 1.0 ± 0.1.

The second-harmonic generation (SHG) experiments were carried out in transmission mode with the laser beam (Nd:YAG, λ = 1064 nm) at an angle of 45° to the LB monolayers. The SHG intensities were calibrated against a Y-cut quartz reference (d_{11} = 0.5 pm V^{-1}). The data of second-harmonic generation (SHG) from the LB monolayers were analyzed by the general procedure described by Ashwell et al.[26]

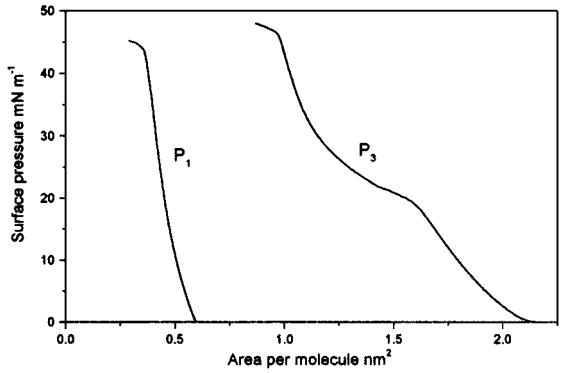

Figure 1. Surface pressure−area ($\pi-A$) isotherms of P_3 and P_1 at the air/water interface (20 ± 1 °C).

Photoelectrochemical measurements were carried out in a 0.5 M KCl solution using the LB monolayer-modified ITO electrode, platinum wire, and Ag/AgCl electrode as working electrode, counter electrode, and reference electrode, respectively. The effective illuminated area of a flat window for P_3 and P_1 was 1 cm^2. The light source used for the photoelectrochemical study was a 500 W Xe arc lamp; the light beam was passed through a group of filters (ca. 400−800 nm, Toshiba Co., Japan, and Schott Co., Germany) in order to get a given band-pass of light. The light intensity at each wavelength was measured with an energy and power meter (Scientech Co., Boulder, CO). Cyclic voltammetric (CV) experiments were performed on an EG&GPAR 273 potentiostat/galvanostat with EG&GPAR 270 electrochemical software.

Results and Discussion

LB Monolayer Properties. The surface pressures versus area isotherms of P_3 and P_1 dyes are shown in Figure 1; data show that the collapse pressures of P_3 and P_1 are 45 and 43 mN m^{-1}, respectively. The limiting molecular area (ca. 0.52 nm^2) of P_1 is slightly larger than that (0.41 nm^2) of the congener *N*-methyl-(4-*N*-methyl-*N*-octadecylamino)styrylpyridinium iodide (P_0) because two methyl groups in the 2,6-positions of the pyrylium ring prevent chromophores from closing up, resulting in a larger separation distance. The isotherm of P_3 appears a plateaulike region from 1.57 to 1.18 nm^2 at 19 mN m^{-1}. Because the ratio of the limiting molecular area at the beginning of the plateau to that at its termination amounts to 1.33, we suggested that such a plateau is not due to the formation of multiplayer but due to a possible phase transition that corresponds to a configurational rearrangement when the surface pressure reaches 19 mN m^{-1}.[27] The limiting areas per molecule of P_3 before and after rearrangement are 2.00 and 1.39 nm^2, respectively, extrapolated to the tangent of the $\pi-A$ curve at 40 and 10 mN m^{-1} (Table 2, A). To discuss conveniently, P_{3a} and P_{3b} stand for LB monolayers of P_3 deposited on quartz (or ITO slides) under 40 and 10 mN m^{-1}, respectively. The limiting molecular area of P_{3a} and P_{3b} are about 5 times and 3 times larger than that of P_0 (0.41 nm), respectively, implying that the three electron-donating groups may be arranged like a half-opened umbrella shape on the substrate with a different tilt angle of 40 and 61° (related to the normal line of the substrate, Table 2, φ). We suggest that P_3 is oriented possibly under 40 and 10 mN m^{-1}, as shown in Scheme 2. Comparing the electronic spectra of LB monolayers with those in chloroform solution (in Table 1, λ_{max}), one observes blue shifts of 40, 37, and 7 nm

TABLE 1: Maximum Absorption for P_{3a}, P_{3b}, and P_1 in Chloroform Solution and in a LB Film

dyes	λ_{max} (nm) in chloroform	λ_{max} (nm)[a] in LB film	$\Delta\lambda_{max}$ (nm)[b]
P_{3a}	690	650	−40
P_{3b}	690	653	−37
P_1	600	593	−7

[a] The absorption peak of the LB film on an ITO electrode is almost the same as that on quartz. [b] "−" indicates a blue shift of the absorption peak of the electric spectrum for the LB film in comparison with that in chloroform solution.

for P_{3a}, P_{3b}, and P_1, respectively, indicating that H-aggregates formed in the monolayers for P_{3a} and P_{3b}.[28] The smaller blue shift of the absorption maximum in LB monolayers $\lambda_{max(f)}$ in comparison with that in solution $\lambda_{max(sol)}$ for the P_1 dye may be attributed to the presence of two methyl groups in 2,6-positions of the pyrylium ring. There is only a slight difference between the spectra of the P_{3a} and P_{3b} LB monolayers, possibly indicating that the change of surface pressure does not affect the relative arrangement of P_3 dye aggregates. Comparing the absorption maximum of P_3 both in solution and in LB monolayers with that of P_1 (Table 1), one observes a red-shift for the P_3 dye due to its larger π-conjugation system.

SHG Properties. The second-harmonic intensities $\chi^{(2)}$ for P_{3a}, P_{3b}, and P_1 LB monolayers deposited on quartz are 236, 67, and 40 pm V^{-1}, respectively. The tilt angles φ of P_{3a}, P_{3b}, and P_1 LB monolayers deposited on quartz are 40, 61, and 31°, respectively. The data show that $\chi^{(2)}$ of P_{3a} is about 6 times larger than that of P_1, implying that the connection of NLO chromophores can improve the SHG property largely. Moreover, it can be seen from the electronic absorption spectra of P_{3a} and P_1 that the resonant enhancement effort of P_3 is weaker than that of P_1. The ratio of the limiting molecular area for P_{3b} and P_{3a} (ca. 1.44) is about equal to the ratio (ca. 1.36) of their cos-(90° − φ), which implies that the difference of the tilt angle for P_{3a} and P_{3b} results mainly from the difference of their limiting molecular area. The data show that $\chi^{(2)}$ of P_{3a} is about 2.63 times larger than that of P_{3b}, indicating that the increasing SHG intensity is not only attributed to the larger number of molecules per unit area but also attributed to the configuration of the molecule when the surface pressure increases from 10 to 40 mN m^{-1}(Table 2, column 7). Therefore, it can be concluded that the configuration of the molecule is an important factor for the SHG property.

Photoelectric Conversion Properties (PEC). A steady cathodic photocurrent was obtained from the P_{3a}, P_{3b}, and P_1 monolayer-modified ITO electrode in 0.5 M KCl solution by illumination of 137 mW cm^{-2} white light (Table 2, I^b). To discuss conveniently, P_{3a} is given as an example for discussion. The photoelectric response of P_{3a} was very stable when switching on and off many times. The action spectrum of the cathodic photocurrent for P_{3a} (see Figure 2b) is similar to the absorption spectrum, suggesting that the P_{3a} monolayers are responsible for photocurrent generation. About 23 nA cm^{-2} photocurrent can be obtained for P_{3a} by a 650 nm light irradiation, which corresponds to an intensity of 4.61×10^{15} photons cm^{-2} s^{-1}, in 0.5 M KCl electrolyte solution with zero bias voltage. The quantum yield is about 0.24% for P_{3a} LB monolayer-modified electrode (in Table 2, η^c) (the absorbance of the monolayers is about 0.61% at 650 nm).

Dependence of PEC on Experimental Conditions. To understand the effect of bias voltage on photoinduced electron injection, the relationship between bias voltage and photoelectric conversion was investigated. Figure 3 shows the dependence of photocurrent on bias voltage. Results show that the cathodic photocurrent for P_{3a} and P_{3b} increases as the negative bias voltage of the electrode increases, indicating that the photocurrent flows in the same direction as the applied negative voltage.

According to Donovan equation,[29] the photocurrent (i) has a dependence on light intensity (I), $i = KI^m$, where $m = 1$ is the characteristic of unimolecular recombination and $m = 1/2$ is the characteristic of bimolecular recombination. The light intensity dependence on the photocurrent measured at a zero bias potential for P_{3a}, P_{3b}, and P_1 LB monolayers on an ITO electrode in 0.5 M KCl electrolyte solution is shown in Figure 4. The equations are (a) $y = 11.16x^{0.71}$, (b) $y = 8.32x^{0.64}$, and (c) $y = 1.06x + 6.26$ ($R^2 = 0.9985$) for P_{3a}, P_{3b}, and P_1, respectively. Comparing these equations with the generally used form, $i = KI^m$, one can see that m values are 0.71, 0.64, and 1 for P_{3a}, P_{3b}, and P_1, respectively, indicating that the separated charge relaxation process occurs in the dyes LB monolayers under unimolecular recombination for the P_1 system and contains both of the above recombination processes for the P_3 system.

It is well-known that the intensity (even the direction) of the photocurrent depends on the nature of the redox couple in the aqueous phase surrounding the electrode. The effects of electron donor and acceptor on the cathodic photocurrent for P_{3a} and P_{3b} and P_1 show that electron acceptors sensitize the cathodic photocurrent and electron donors (H_2Q and N_2) quench it (even reverse it) and all level off at a certain concentration (in Table 3). Figure 5 is a plot of the photocurrent for P_{3a} versus the concentration of $EuCl_3$ illustrated by the white light at 102 mW cm^{-2} and without any bias voltage, in 0.5 M KCl electrolyte solution. The cathodic photocurrent increased gradually with increasing the concentration of $EuCl_3$ and leveled off at 3.5 mM. This means that $EuCl_3$ acted as a supersensitizer in accepting electrons from the P_{3a} assemblies and therefore increased the concentration of electrons involved in the electron-transfer process. A photocurrent of 37.4 nA cm^{-2} for P_{3a} was obtained under the irradiation at 650 nm; the quantum yield is 0.48%. Under favorable conditions, such as irradiation under 650, 650, and 600 nm wavelength monochromatized from 137 mW cm^{-2} white light, which corresponds to an intensity 4.61×10^{15}, 4.61×10^{15}, and 5.27×10^{15} photons cm^{-2} s^{-1} for P_{3a}, P_{3b}, and P_1, respectively, under −100 mV, dissolved O_2, 2 mM MV^{2+}, and 4 mM Eu^{3+}, the quantum yields are 1.21, 0.53, and 0.42%, respectively (see Table 2, η^d).

Correlation between Molecular Structure and PEC Property. The data of photocurrent per square centimeter (Table 2, I) and external quantum yield (Table 2, η) apparently reveal that the PEC properties of P_{3a} are better than those of P_{3b} and P_1. Although the number of active moieties per unit area in the LB monolayers is an important factor contributing to the PEC performance, in these cases, the effects of structural variations play the key role in the differences of the PEC properties for P_{3a}, P_{3b}, and P_1. To discuss conveniently, we assume that the (D-π)$_3$-A molecule (P_3) contains three D-π-A chromophores. Taking the limiting molecular area into account, one can get the molecular number per square centimeter as 7.19×10^{13} and 1.92×10^{14} for P_{3a} and P_1 [Table 2, no.(m)], respectively. Consequently, the chromophore numbers per square centimeter for P_{3a} and P_1 are 2.15×10^{14} and 1.92×10^{14} [Table 2, no.-(c)], respectively. Furthermore, with reference to the photocurrent per square centimeter, one can see that the photocurrents per one chromophore for P_{3a} and P_1 are 1.64×10^{-12} and 7.27×10^{-13} nA chromophore^{-1} (Table 2, I_2^b), respectively. Therefore, the photcurrent per one P_{3a} molecule ($3 \times 1.64 \times 10^{-12}$ nA cm^{-2}) is about 2 times larger than the photocurrent

TABLE 2: Data of P_{3a}, P_{3b}, and P_1 LB Film Properties[a]

dye	I,[b] nA cm^{-2}	I^c	η,[c] %	I,[d] nA cm^{-2}	η,[d] %	$\chi^{(2)}$, pm V^{-1}	φ, deg	A, nm^2	no.(m), 10^{14} cm^{-2}	I_1,[b] 10^{-12} nA molecule^{-1}	no.(c), 10^{14} cm^{-2}	I_2,[b] 10^{-12} nA chromophore^{-1}
P_{3a}	354.0	23	0.24	118	1.21	236	40	1.39	0.72	4.92	2.15	1.64
P_{3b}	194.5	13	0.11	62.5	0.53	65	61	2.00	0.50	3.89	1.50	1.30
P_1	139.5	8.5	0.09	39.4	0.42	40	31	0.52	1.92	0.73	1.92	0.73

[a] I = photocurrent per square centimeter; I_1 = photocurrent per molecule; I_2 = photocurrent per chromophore; η = external quantum yield; $\chi^{(2)}$ = second-harmonic intensity; φ = tilt angle relative to the normal line on the substrate; A =limiting area per molecule; no.(m) = molecule number per square centimeter; no.(c) = chromophore number per square centimeter. P_{3a} and P_{3b} stand for P_3 LB film deposited under 40 and 10 mN m^{-1}, respectively. [b] Irradiation under 137 mW cm^{-2} white light for P_{3a}, P_{3b}, and P_1, respectively, in 0.5 M KCl electrolyte solution containing dissolved O_2. [c] Irradiation under 137 mW cm^{-2} white light at 650, 650, and 600 nm for P_{3a}, P_{3b}, and P_1, respectively, in 0.5 M KCl electrolyte solution containing dissolved O_2. [d] Irradiation under 137 mWcm^{-2} white light at 650, 650, and 600 nm for P_{3a}, P_{3b}, and P_1, respectively, under −100 mV, dissolved O_2, 2 mM MV^{2+}, and 4 mM Eu^{3+}.

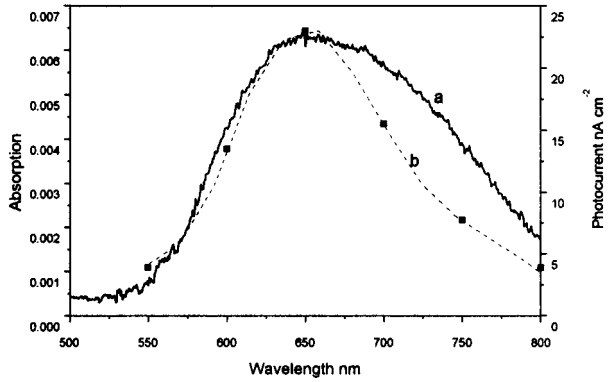

Figure 2. UV-vis absorption spectrum (a) of P_{3a} in LB monolayers and action spectrum (b) of the cathodic photocurrents for P_{3a}. The intensities of different wavelengths are all normalized.

SCHEME 2: The Possible Arrangement of P_{3a} and P_{3b} at the Air/Water Interface

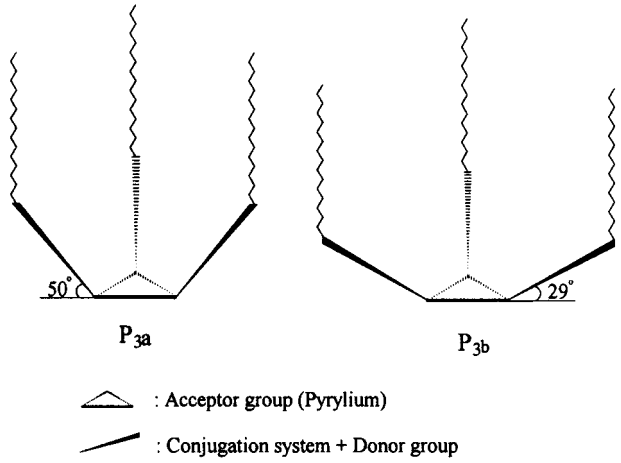

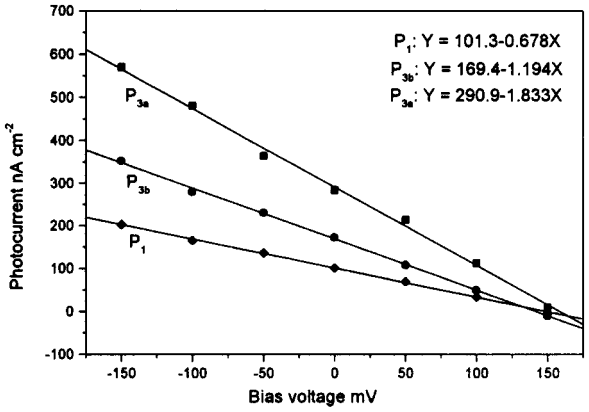

Figure 3. Photocurrent versus bias voltage for P_{3a}, P_{3b} and P_1 LB film-ITO electrodes in 0.5 M KCl aqueous solution under ambient conditions, upon irradiation of 102 mWcm^{-2} white light.

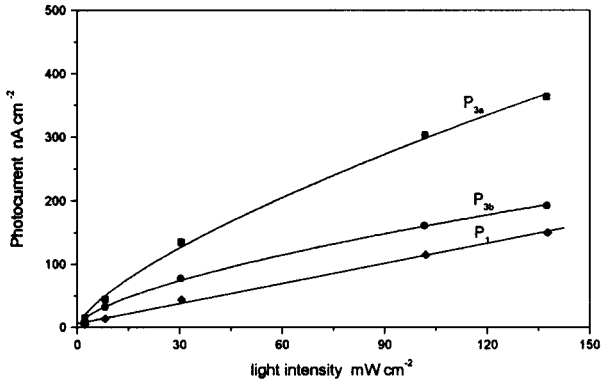

Figure 4. Dependence of the photocurrent upon light intensity for P_{3a}, P_{3b} and P_1 electrodes in 0.5 M KCl electrolyte solution under ambient condition without bias voltage.

per three P_1 molecules ($3 \times 7.27 \times 10^{-13}$ nA cm^{-2}). This is another system for $1 + 1 + 1 > 3$.[15] Apparently, P_{3a} performs better in photocurent generation than P_1 does, which is mainly due not to the larger number of chromophores per square centimeter but to the different connection of the chromophores. The reasons for this interesting phenomenon are being studied. Comparing the data of P_{3a} with those of P_{3b} shows the photocurrent per P_{3a} molecule (4.92×10^{-12} nA cm^{-2}) is larger than that for P_{3b} (3.89×10^{-12} nA cm^{-2}) (see Table 2), indicating that the decreasing tilt angle (relative to the normal line of the substrate) results in the increasing photocurrent when the surface pressure is increased from 10 to 40 mN m^{-1}, which implies the configurational change plays an important role in photocurrent generation.

Electrochemical Properties of the Dyes. To estimate the energy level of the excited-state dye and to discuss the mechanism of photocurrent generation, CV studies for the three dyes were carried out (sweep rate = 100 mV s^{-1}) in 0.1 M KCl aqueous solution. Oxygen was removed from the electrolyte solution by bubbling N_2 before every measurement. The CV graphs of P_{3a}, P_{3b}, and P_1 monolayers modified on ITO electrodes show similar shapes, indicating that the electrochemical behavior of the LB monolayers on the ITO electrode are identical for these dyes. The oxidation peak potentials are 0.25, 0.24, and 0.21V for P_{3a}, P_{3b}, and P_1, respectively.

Mechanism of Photoelectric Conversion. According to the Franck−Condon principle, the only possibility for generating photocurrent under these circumstances is photoinduced electron transfer between the ITO substrate and the excited-state dye within the LB monolayers. To elucidate the mechanism of the photoinduced electron-transfer process for the cathodic and anodic photocurrent, the energy levels of the relevant

TABLE 3: Effect of Donors and Acceptors on the Photoelectric Conversion of P_{3a} Monolayer LB Film Modified ITO Electrode

		photocurrent (nA cm^{-2})[a]	
donor/acceptor	concentrated mm	ambient	N_2 degassed
MV^{2+}	0	295	46
	4	634	168
Eu^{3+}	0	274	40
	3.5	684	147
H_2Q	0	284	38
	5.4	−308[b]	−961

[a] irradiation under 102 mW cm^{-2} white light for P_{3a} in 0.5 M KCl electrolyte solution. [b] "-" stands for anoxic photocurrent.

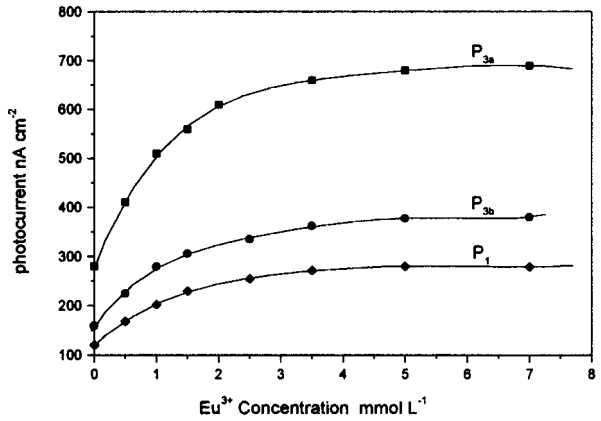

Figure 5. Dependence of the photocurrent on the concentration of $EuCl_3$ under ambient conditions for P_{3a}, P_{3b} and P_1monolayer upon irradiation with 102 mW cm^{-2} white light.

electronic states must be estimated. The oxidation peak potential for the dyes provides a measurement of the energy of the HOMO. The energy levels of the excited state for P_{3a}, P_{3b}, and P_1 LB films are −4.99 eV (0.25 V vs SCE), −4.98 eV (0.24 V vs SCE), and −4.95 eV (0.21 V vs SCE) on the absolute scale, respectively. With reference to UV−vis spectra of P_{3a}, P_{3b}, and P_1 LB monolayers, their $\lambda_{max(f)}$ are 650, 653, and 593 nm and their band gaps are 1.91, 1.90, and 2.09 eV, respectively. Therefore, the energy levels of the ground state for P_{3a}, P_{3b}, and P_1 LB monolayers are −3.08, −3.08, and −2.86 eV on the absolute scale, respectively. The conduction band (E_c) and valence band (E_v) edges of the ITO electrode surface are estimated to be ca. −4.5 and −8.3 eV,[30] respectively. The reduction potential of MV^{2+} is −4.51 eV (−0.23 V vs SCE),[31] the reduction potential of Eu^{3+} is −4.43 eV (−0.31 V vs SCE), and the oxidation potential of H_2Q is −4.61 eV (−0.13 V vs SCE),[31] on the absolute scale. Then, an energy level diagram for P_{3a}, P_{3b}, and P_1 only can be constructed; that for P_{3a} is shown in Scheme 3 only for clarity, which describes the mechanism for photosensitization of the ITO electrode.

It can be known from the energy level that the direction of the photocurrent depends not only on the dye sensitized by the light but also on the nature of the redox couple in the aqueous phase surrounding the electrode solution. In the presence of some electron acceptors, such as O_2, MV^{2+}, and Eu^{3+} in electrolyte solution, an electron transfers from the excited state of P_{3a} to the electron acceptor; subsequently, the electrons of ITO conduction band inject into the hole residing in the dye molecules. Thus, cathodic photocurrent is generated. On the contrary, if there are strong electron donors in the system, such as H_2Q, it will exhibit a reduced photocurrent even in the reverse direction of the photocurrent.

SCHEME 3: Schematic Diagram Showing Electron Transfer Processes[a]

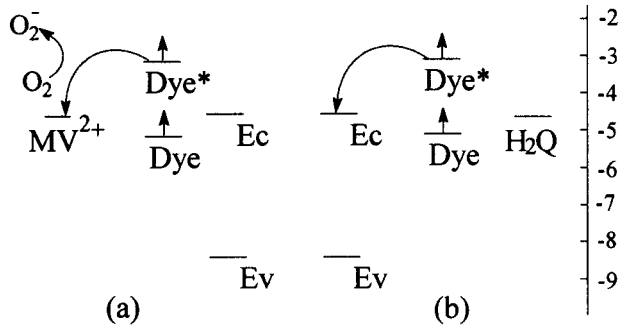

[a] (a)cathodic photocurrent; (b) anodic photocurrent. Dye and Dye* present the ground state and excited state of the dye P_{3a}, respectively.

Conclusions

It can be seen from the Table 2 that in the present systems the second-harmonic generation intensity $\chi^{(2)}$ and photocurrent quantum yield η have the same sequence under the same conditions: $P_3 > P_1$. The experimental results of photocurrent generation show that the two-dimensional $(D\text{-}\pi)_3$-A dye molecule (P_3) exhibits a photocurrent per one P_3 molecule (4.92×10^{-12} nA cm^{-2}) 3 times larger than the dipolar one-dimensional D-π-A molecule (P_1) does (7.27×10^{-13} nA cm^{-2}) when they are deposited under 40 mN m^{-1}. It exhibits an interesting phenomenon: $1 + 1 + 1 > 3$. Moreover, the second-harmonic generation and photocurrent generation of P_3 monolayers deposited under different surface pressures before (10 mN m^{-1}) and after (40 mN m^{-1}) the plateau of its $\pi-A$ isotherm is greatly changed, which indicates that the molecular configurational rearrangement affects greatly its SHG and PEC properties.

Acknowledgment. The authors thank the State Key Project of Fundamental Research (G1998061310 and G1998061322) and National Natural Science Foundation of China for financial support of this work.

References and Notes

(1) Marder, S. R.; Perry, J. W. *Adv. Mater.* **1993**, *5*, 804.
(2) Jen, A. K. Y.; Wu, X.; Ma, H. *Chem. Mater.* **1998**, *10*, 471.
(3) Jen, K. Y.; Cai, Y.; Bedworth, P. V.; Marder, S. R. *Adv. Mater.* **1997**, *9*, 132.
(4) Lacroix, P. G.; Clément, R.; Nakatani, K.; Zyss, J.; Ledoux, I. *Science* **1994**, *263*, 658.
(5) Benard, S.; Yu, P.; Coradin, T.; Rivière, E.; Nakatani, K.; Clément, R. *Adv. Mater.* **1997**, *9*, 981.
(6) Lacroix, P. G.; Nakatani, K. *Adv. Mater.* **1997**, *9*, 1105.
(7) Andreu, R.; Malfant, I.; Lacroix, P. G.; Gornitzka, H. *Chem. Mater.* **1999**, *11*, 840.
(8) Cheng, L. T.; Tam, W.; Stevenson, S. H.; Meridith, G. R.; Rikken, G.; Marder, S. R. *J. Phys. Chem.* **1991**, *95*, 10631.
(9) Kanis, D. R.; Ratner, M. A.; Marks, T. J. *Chem. Rev.* **1994**, *94*, 195.
(10) *Nonlinear Optical Materials. Theory and Modeling*; Karna, S. P., Yeates, A. T., Eds.; ACS Symposium Series 628; American Chemical Society: Washington, DC, 1996.
(11) Zyss, J. *Nonlinear Opt.* **1991**, *1*, 3.
(12) Zyss, J.; Ledoux, I. *Chem. Rev.* **1994**, *94*, 77.
(13) Dhenaut, C.; Ledoux, I.; Samuel, D. W.; Zyss, J.; Bourgault, M.; LeBozec, H. *Nature* **1995**, *374*, 339.
(14) Wolff, J. J.; Längle, D.; Hillenbrand, D.; Wortmann, R.; Matschiner, R.; Glania, C.; Krämer, P. *Adv. Mater.* **1997**, *9*, 138.
(15) Wu, D. G.; Huang, C. H.; Zhang, W.; Gan, L. B.; Zheng, J.; Luo, H. X.; Li, N. Q. *J. Phys. Chem. B* **1999**, *103*, 4377.
(16) Dirk, C. W.; Twing, R. J.; Wagniere, G. *J. Am. Chem. Soc.* **1986**, *108*, 5397.
(17) Lang, A. D.; Zhai, J.; Huang, C. H.; Gan, L. B.; Zhao, Y. L.; Zhou, D, J.; Chen, Z. D. *J. Phys. Chem. B* **1998**, *102*, 1424.
(18) Xia, W. S.; Huang, C. H.; Luo, C. P.; Gan, L. B. *J. Phys. Chem.* **1996**, *100*, 15525.

(19) Xia, W. S.; Huang, C. H.; Gan, L. B.; Li, H. *J. Chem. Soc., Faraday Trans.* **1996**, *92*, 3131.
(20) Xia, W. S.; Huang, C. H.; Zhou, D. J. *Langmuir* **1997**, *13*, 80.
(21) Zhai, J.; Huang, C. H.; Wei, T. X.; Yu, A. C.; Zhao, X. S. *Solid-State Commun*. **1999**, *109*, 733.
(22) Wu, D. G.; Huang, C. H.; Gan, L. B.; Huang, Y. Y. *Langmuir* **1998**, *14*, 3783.
(23) Wu, D. G.; Huang, C. H.; Huang, Y. Y.; Gan. L. B.; Yu, A. C.; Ying, L. M.; Zhao, X. S. *J. Phys. Chem. B* **1999**, *103*, 7130.
(24) Wang, H.; Xu, L.; Zhang, B.; Cao, Y. *Chem. Res. China* **1997**, *8* (4), 1.
(25) Hauser, H.; Kaiser, H. *Organic Synthesis*; Wiley: New York, 1973; Collect. Vol. 5, p 1112.
(26) Ashwell, G. J.; Jackson, P. D.; Lochum, D.; Crossland, W. A.; Thrompson, P. A.; Bahra, G. S.; Brown, C. R.; Jasper, C. *Proc. R. Soc. London A* **1994**, *445*, 385.
(27) Roberts, G. *Langmuir*−*Blodgett Monolayers*; Plenum Press: New York, 1990; Chapter 2.
(28) Mooney, W. F.; Brown, P. E.; Russell, J. C.; Costa, S. B.; Pedersen, L. G.; Whitten, D. G. *J. Am. Chem. Soc.* **1984**, *106*, 5659.
(29) Donovan, K. J.; Sudiwala, R. V.; Wilson, E. G. *Mol. Cryst. Liq. Cryst.* **1991**, *194*, 337.
(30) Sereno, L.; Silber, J. J.; Otero, L.; Bohorquez, M. D. V.; Moore, A. L.; Moore, T. A.; Gust, D. *J. Phys. Chem.* **1996**, *100*, 814.
(31) Kim, Y. S.; Liang, K.; Law, K. Y.; Whitten, D. G. *J. Phys. Chem.* **1994**, *98*, 984.